 CMC, vol.46, no.1, pp.1-16, 2015

# Fracture Mechanics Approach to Estimate Fatigue Lives of Welded Lap-Shear Specimens

[1]Poh-Sang Lam[2] and Jwo Pan[3]

**Abstract:** A full range of stress intensity factor solutions for a kinked crack with finite length is developed as a function of weld width and the sheet thickness. When used with the main crack solutions (global stress intensity factors) in terms of the applied load and the specimen geometric parameters, the fatigue lives of the kinked crack can be estimated for the laser-welded lap-shear specimens. The predicted curve for the load range-fatigue life passes through the cluster of experimental data and is in good agreement. A classical solution associated with an infinitesimal kink is also employed. However, its life prediction tends to overestimate the actual fatigue life. In addition, the traditional fatigue life estimation based on structural stress is performed for completeness. This non-fracture mechanics approach only agrees well with the experimental data under high cyclic load conditions.

**Keywords:** Kinked crack, stress intensity factor, lap-shear, weld, fatigue life, Paris law.

## 1 Introduction

This paper is a summary of recent development at the University of Michigan for estimating fatigue life of laser weld in a lap-shear specimen [e.g., the work of Sripichai et al. (2011); Asim et al. (2014)]. The specimens were made of thin sheets of SAE J2340 300Y High Strength Low Alloy (HSLA) steel and were welded with 6 kW $CO_2$ laser. When a specimen was subjected to cyclic loading

[1] This manuscript has been authored by Savannah River Nuclear Solutions, LLC under Contract No. DEAC09- 08SR22470 with the U.S. Department of Energy. The United States Government retains and the publisher, by accepting this article for publication, acknowledges that the United States Government retains a non-exclusive, paid-up, irrevocable, worldwide license to publish or reproduce the published form of this work, or allow others to do so, for United States Government purposes.

[2] Materials Science & Technology, Savannah River National Laboratory, Aiken, South Carolina, U.S.A.

[3] Department of Mechanical Engineering, University of Michigan, Ann Arbor, Michigan, U.S.A.

conditions, two main cracks were formed on each side of the weld. The lap-shear load is statically equivalent to a combined loading of a membrane force and a bending moment. The beam theory is used to calculate the structural stress as experienced at the edges of the weld. The structural stress represents the sum of the uniform normal stress on the cross-section of the specimen due to the membrane force and the maximum normal stress on the cross-section due to the bending moment at the edges of the weld. The principle of superposition is employed to decompose the loading system into several simpler configurations to facilitate the derivation of the stress intensity factors in crack opening mode ($K_{\mathrm{I}}$) and sliding mode ($K_{\mathrm{II}}$).

The fatigue lives of the lap-shear specimens can be estimated by three approaches:

(1) With the structural stresses calculated from the beam theory, the fatigue lives can be estimated with the experimental fatigue data of the material, typically known as the $S-N$ curve (stress vs. number of cycles);

(2) The fatigue life can be obtained by integrating the empirical Paris law ($da/dN = C(\Delta K)^m$), where $a$ is the crack length, $N$ is the number of cycles, $\Delta K$ is the loading characterized by the range of stress intensity factors, and $C$ and $m$ are material constants obtained by curve-fitting. The key for this approach is that the stress intensity factor solutions must be known. From the lap-shear specimen fatigue testing, it is noted that a kinked crack is formed at the main crack tip and propagates through the sheet thickness leading to failure. Therefore, two sets of stress intensity factors must be determined: 1) for the main crack and 2) for the kinked crack. The stress intensity factors for the main crack were obtained by previous work such as Sripichai et al. (2011). The solution process will be summarized in this paper. A theoretical solution of the stress intensity factors for a kinked crack has been derived by Cotterell and Rice (1980). These solutions can be used with the Paris law and a simple equation for fatigue life can be obtained by direct integration; and

(3) As the kinked crack grows eventually leading to failure, the stress intensity factor solutions of Cotterell and Rice for an infinitesimal kinked crack become inadequate. A set of finite element based solutions must be used with the Paris law.

This paper will describe the essential elements of these approaches. The estimations will be compared with the experimental data.

## 2 Specimen Configuration

A welded lap-shear specimen is schematically shown in Fig. 1, in which $W$= 27mm, $b$= 8 mm, $c$= 13.5 mm, $w$= 1 mm, $L$= 95 mm, $V$= 30 mm, $t$= 0.93 mm, $r$= 10 mm, and $s$= 50 mm. The cyclic load $F$ is applied to both ends of the specimen. A detailed weld configuration is shown in Fig. 2. Figure 3 shows the welded region of the test specimen prior to final failure by the cyclic load. Note that the kinked

crack on the right is longer than the one on the left. The Young's modulus, yield strength, and tensile strength of the HSLA steel are, respectively, 206 GPa, 315 MPa, and 415 MPa. The hardening exponent is 0.15 and the strength coefficient is 633 MPa.

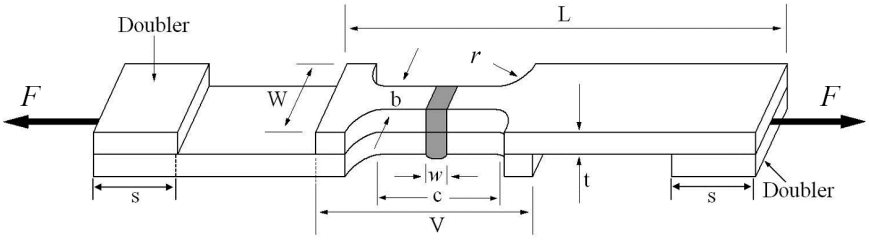


Figure 1: A schematic of a lap-shear specimen.

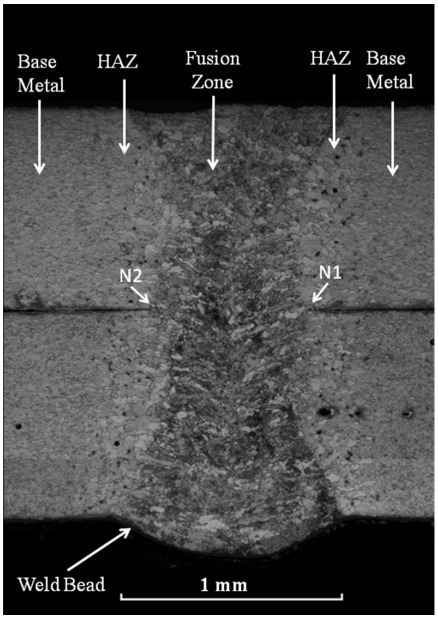


Figure 2: Weld details.

## 3 Principle of Superposition – Global Stress and Stress Intensity Factors

Radaj (1989), Radaj and Zhang (1991a, 1991b, 1992), Lin et al. (2007), and Lin and Pan (2008) showed that the load $F$ of a lap-shear specimen (Fig. 4a) can be de-

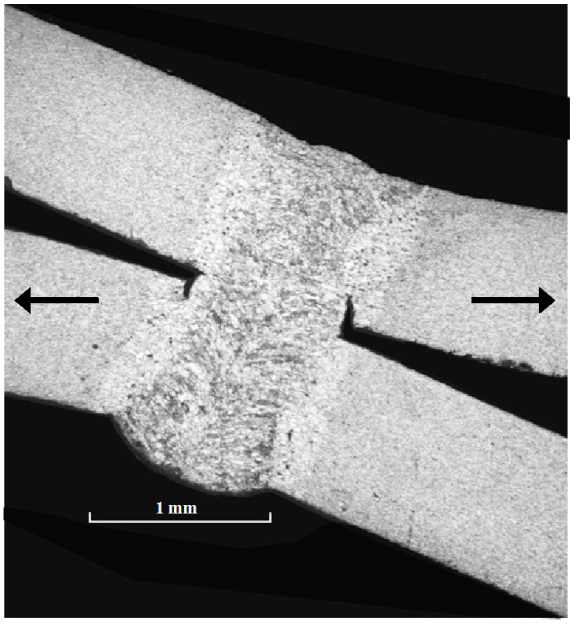


Figure 3: A partially failed laser weld. Note that the right kinked crack is always longer and the upper right leg always separates under high cycle fatigue testing.

composed into statically equivalent symmetric and anti-symmetric loads. The dog-bone area (mid-section) of a lap-shear specimen is modeled as two beams which are connected by the weld (Fig. 4b). It can be seen that the equivalent loadings are the membrane force per unit width ($F/b$) and the bending moment per unit width ($Ft/2b$), applied at the middle surfaces of the upper or the lower beams.

The loading in Fig. 4b can further be decomposed into four symmetric and anti-symmetric loading conditions: counter bending (Fig. 4c), central bending (Fig. 4d), tension (Fig. 4e), and in-plane shear (Fig. 4f). The bending moments per unit width of the counter bending and central bending loading conditions have a magnitude of $Ft/4b$, and the forces per unit width of the tension and in-plane shear loading conditions are $F/2b$.

### *3.1 Global Structural Stress at Weld Edge*

From Fig. 4b, the structural stress in the lap-shear specimen can be easily shown as

$$\sigma = \frac{F}{tb} + \frac{3F}{tb} \tag{1}$$

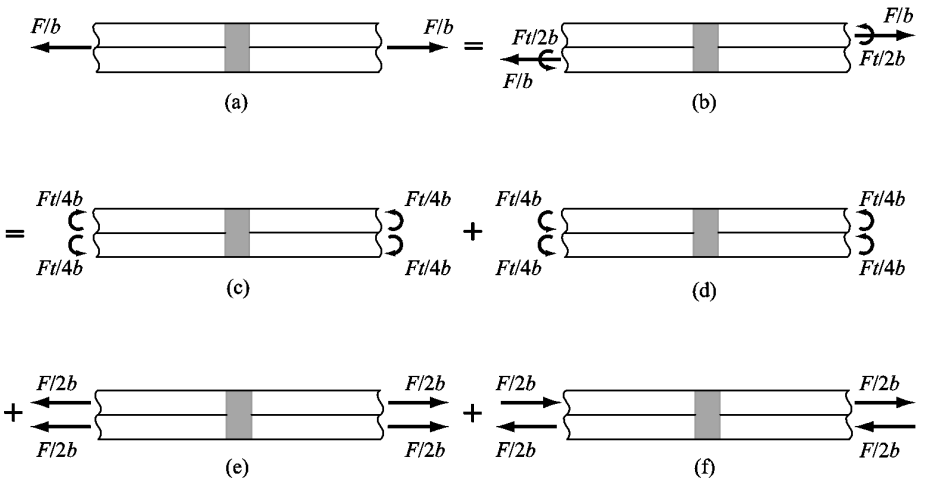


Figure 4: Decomposition of the lap-shear loading system. The shaded area is the weld zone. The two-beam model is subjected to the lap-shear loading as shown in (a), which is equivalent to the loading in (b). By superposition, (b) is the sum of (c) counter bending, (d) central bending, (e) tension, and (f) in-plane shear loading.

Note that the first term on the right hand side of Eq. 1 corresponds to the membrane force per unit width and the second term is from the bending moment per unit width. With Eq. (1) defined as the cyclic structural stress at the edge of the weld bead and utilizing the experimental stress-fatigue life data ($S-N$ Curve) of the HSLA steel, the fatigue lives of laser welds in lap-shear specimens can be estimated.

### *3.2 Global Stress Intensity Factors for the Main Cracks*

In terms of linear elastic fracture mechanics, the crack driving force ($G$) or the energy release rate of a crack is the decrease of potential energy per unit crack extension. In addition, it has been shown that the energy release rate and the stress intensity factors are related by

$$G = \frac{K_{\mathrm{I}}^2 + K_{\mathrm{II}}^2}{E'} \tag{2}$$

where $E' = E/(1-\nu^2)$ for plane strain and $E' = E$ for plane stress, $E$ is the Young's modulus, and $\nu$ is the Poisson's ratio. Based on these conditions, Sripichai et al. (2011) showed that the stress intensity factors with respect to the decomposed configurations are:

(i) Figure 4c, Counter Bending

$$K_{\mathrm{I,B}} = \frac{\sqrt{3}}{2}\frac{F}{b\sqrt{t}}$$

$$K_{\mathrm{II}} = 0$$

*(ii) Figure 4d, Central Bending*

$$K_{\mathrm{I}} = 0$$

$$K_{\mathrm{II,CB}} = \frac{3}{4}\frac{F}{b\sqrt{t}}$$

(iii) Figure 4e, Simple Tension along the Crack Face

$$K_{\mathrm{I}} = K_{\mathrm{II}} = 0$$

(iv) Figure 4f, In-plane Shear

$$K_{\mathrm{I}} = 0$$

$$K_{\mathrm{II,S}} = \frac{F}{4b\sqrt{t}}$$

Therefore, by superposition, the "global" stress intensity factors for the main cracks of the lap-shear specimen subject to load $F$ (Fig. 1) are

$$K_{\mathrm{I}} = K_{\mathrm{I,B}} = \frac{\sqrt{3}}{2}\frac{F}{b\sqrt{t}} \tag{3}$$

$$K_{\mathrm{II}} = K_{\mathrm{II,CB}} + K_{\mathrm{II,S}} = \frac{F}{b\sqrt{t}} \tag{4}$$

Note that Eqs. (3) and (4) are valid only when the weld width $w$ is large compared to the sheet thickness $t$. When $w$ becomes smaller, the Westergaard stress function solutions in Tada et al. (2000) prevail:

$$K_{\mathrm{I,TPI}} = 0$$

$$K_{\mathrm{II,TPI}} = \frac{\sqrt{2F}}{b\sqrt{\pi w}}$$

To obtain the full range of the global stress intensity factor as a function of $w/t$, the finite element analysis was carried out by Sripichai et al. (2011). Their approximate solutions for $K_{\mathrm{I}}$ and $K_{\mathrm{II}}$ are given as (also shown graphically in Fig. 5):

(a) Solution for $K_{\mathrm{I}}$

$$\begin{aligned} &\text{(i) For } \ 0 \le w/t < 2, \ \ K_{\mathrm{I}} = \frac{\sqrt{3}}{2}\frac{F}{b\sqrt{t}}\frac{w}{2t} \\ &\text{(ii) For } \ w/t \ge 2, \ \ K_{\mathrm{I}} = \frac{\sqrt{3}}{2}\frac{F}{b\sqrt{t}} \end{aligned} \tag{5}$$

(b) Solution for $K_{\mathrm{II}}$

$$\begin{aligned} &\text{(i) For } \ 0 \le w/t < 0.37, \ \ K_{\mathrm{II}} = K_{\mathrm{II,TPI}} = \frac{\sqrt{2}F}{b\sqrt{\pi w}} \\ &\text{(ii) For } \ 0.37 \le w/t < 1.12, \ \ K_{\mathrm{II}} = 1.0285\left(\frac{w}{t}\right)^{-0.242}\frac{F}{b\sqrt{t}} \\ &\text{(iii) For } \ w/t \ge 1.12, \ \ K_{\mathrm{II}} = \frac{F}{b\sqrt{t}} \end{aligned} \tag{6}$$

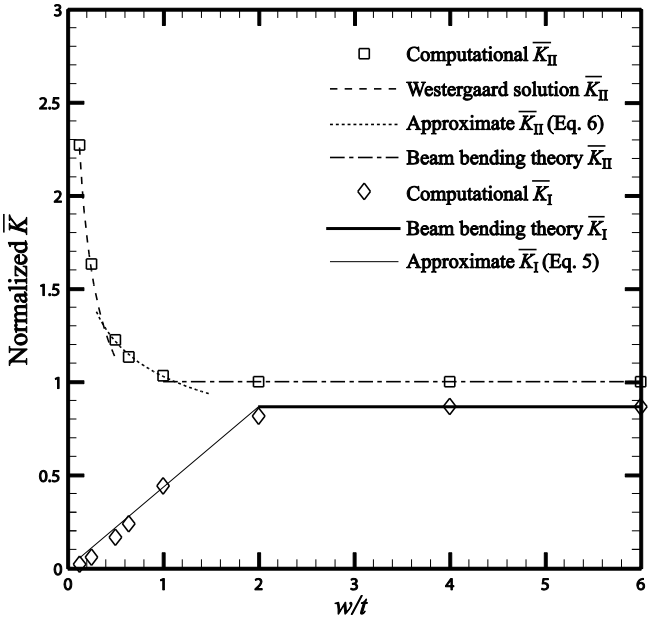


Figure 5: The global stress intensity factors as functions of $w/t$ (all $K_{\mathrm{I}}$'s and $K_{\mathrm{II}}$'s are normalized by Eq. (4)).

### 3.3 Stress Intensity Factors for the Kinked Crack

#### 3.3.1 Analytical Solution

In reality, the experimental observation suggested that the fatigue cracks of the lap-shear specimens never follow the direction of the main cracks (formed by the two sheets and the weld). Instead, as shown in Fig. 3, a kinked crack was initiated at each of the main crack tips. Figure 6 is a schematic of a kinked crack with length $a$ and a kink angle $\alpha$. Denoting $K_{\mathrm{I}}$ and $K_{\mathrm{II}}$ as the global stress intensity factors for the main crack, the solutions for the local stress intensity factors $k_{\mathrm{I}}$ and $k_{\mathrm{II}}$ for the kinked crack are given by Bilby et al. (1978) and Cotterell and Rice (1980):

$$(k_{\mathrm{I}})_0 = \frac{1}{4}\left(3\cos\frac{\alpha}{2}+\cos\frac{3\alpha}{2}\right)K_{\mathrm{I}} - \frac{3}{4}\left(\sin\frac{\alpha}{2}+\sin\frac{3\alpha}{2}\right)K_{\mathrm{II}} \tag{7}$$

$$(k_{\mathrm{II}})_0 = \frac{1}{4}\left(\sin\frac{\alpha}{2}+\sin\frac{3\alpha}{2}\right)K_{\mathrm{I}} + \frac{1}{4}\left(\cos\frac{\alpha}{2}+3\cos\frac{3\alpha}{2}\right)K_{\mathrm{II}} \tag{8}$$

where $(k_{\mathrm{I}})_0$ and $(k_{\mathrm{II}})_0$ represent the local $k_{\mathrm{I}}$ and $k_{\mathrm{II}}$ solutions for the kinked crack with its length $a$ approaching to 0 (i.e., an infinitesimal kink). Note that the arrows in Fig. 6 indicate the positive sense of the stress intensity factors $K_{\mathrm{I}}$, $K_{\mathrm{II}}$, $k_{\mathrm{I}}$, and $k_{\mathrm{II}}$.

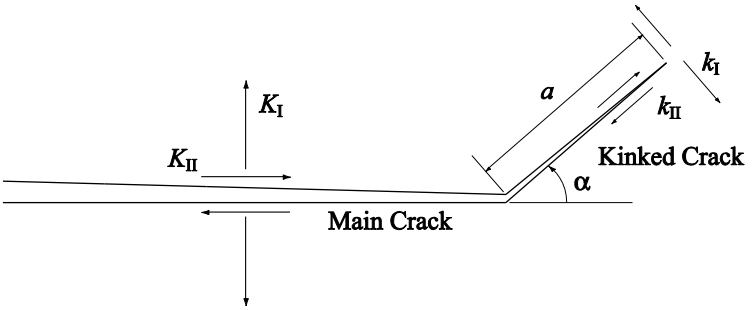


Figure 6: A schematic of a main crack and a kinked crack with kink length $a$ and kink angle $\alpha$.

#### 3.3.2 Numerical Solutions for a finite kinked Crack

Note that the theoretical solutions for a kinked crack in Eqs. (7) and (8) are functions of the kink angle $\alpha$ and the specimen overall geometry (through the global stress intensity factors $K_{\mathrm{I}}$ and $K_{\mathrm{II}}$), and is independent of the kink length $a$. However, as the kinked crack continues to grow under fatigue load, it is expected that the

local stress intensity factors ($k_{\mathrm{I}}$ and $k_{\mathrm{II}}$) will increase with the kink length. Therefore, finite element analysis was conducted by considering that the kinked crack has a finite length. In addition, for the particular lap-shear specimens discussed in this paper, the kink is assumed to be perpendicular to the main crack (i.e., $\alpha = -90^{\circ}$) as shown in Fig. 3. The finite element model is schematically shown in Fig. 7 and the calculated stress intensity factors $k_{\mathrm{I}}$ and $k_{\mathrm{II}}$, which both are normalized by $(k_{\mathrm{I}})_0$ for convenience, are plotted in Figs. 8 and 9.

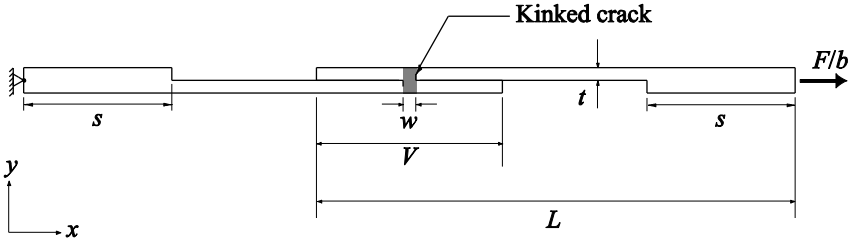


Figure 7: A schematic of a two-dimensional finite elemental model of a lap-shear specimen with two kinked cracks.

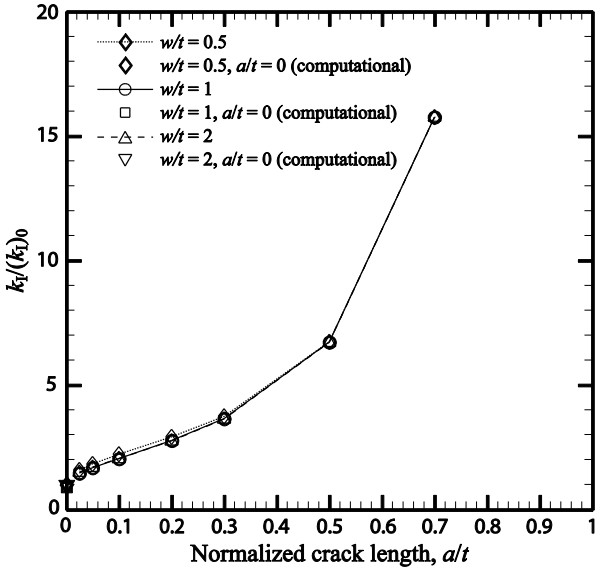


Figure 8: The values of $k_{\mathrm{I}}/\left(k_{\mathrm{I}}\right)_0$ for $w/t$=0.5, 1, and 2 with $\alpha = -90^{\circ}$.

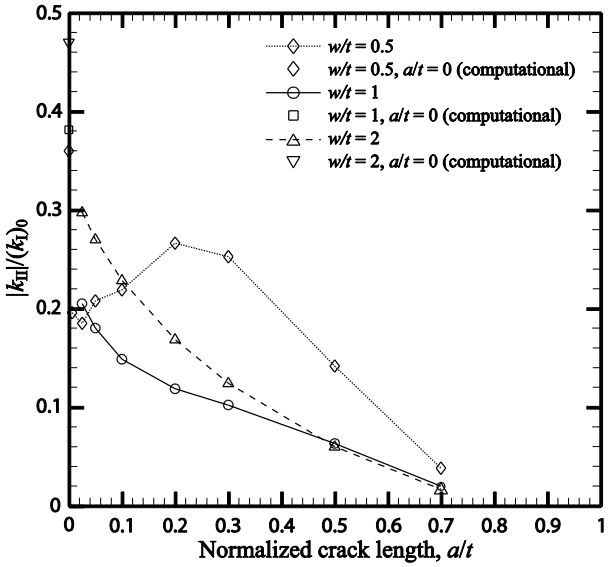


Figure 9: The values of $k_{\mathrm{II}}/(k_{\mathrm{I}})_0$ for $w/t$=0.5, 1, and 2 with $\alpha = -90^{\circ}$.

## 4 Estimation of Fatigue Life

The fatigue life of a structural component can be estimated based on: 1) structural stress, using the fatigue data from material testing, typically known as the $S-N$ Curve, and 2) fracture mechanics, using the stress intensity factor solutions at the tip of a fatigue crack.

### *4.1 Structural Stress Model*

The structural stress for the welded lap-shear specimen was derived in Section 3.1 as $\sigma = F/tb + 3F/tb = 4F/tb$ (Eq. (1)). With the applied stress ($\sigma$) and the $S-N$ fatigue curve for HSLA steel, the fatigue life curve can be constructed. However, the stress-life data for the SAE 300Y HSLA (with the tensile yield strength of 315 MPa) are not available, and the stress-life data for $R = -1$ of SAE 950X (with the tensile yield strength of 350 MPa) are used instead. The fatigue life estimations with the structural stress are plotted against the experimental data in Fig. 10.

### *4.2 Fatigue Crack Growth Model*

Here the Paris law ($da/dN = C(\Delta K)^m$) is adopted to describe the fatigue crack propagation for kinked cracks emanating from the main cracks in the lap-shear

specimens. Because both $k_{\mathrm{I}}$ and $k_{\mathrm{II}}$ exist at the crack tip, an equivalent stress intensity factor range ($\Delta k_{\mathrm{eq}}$) is used. The Paris law is rewritten as

$$\frac{da}{dN} = C\left(\Delta k_{\mathrm{eq}}(a)\right)^m \tag{9}$$

where

$$\Delta k_{\mathrm{eq}}(a) = \sqrt{\Delta k_{\mathrm{I}}(a)^2 + \gamma \Delta k_{\mathrm{II}}(a)^2} \tag{10}$$

In the above equation, $\gamma$ is an empirical constant to account for the sensitivity of material to the Mode II loading conditions. In the absence of information, the value of $\gamma$ is simply taken as unity (1). By substituting Eq. (10) into Eq. (9) and integrating, the fatigue life of a laser weld in lap-shear specimens can be expressed as

$$N = \frac{1}{C}\left[\int_0^{0.025t'} \left[\Delta k_{\mathrm{eq}}(a)\right]^{-m} da + \int_{0.025t'}^{0.05t'} \left[\Delta k_{\mathrm{eq}}(a)\right]^{-m} da + \ldots + \int_{0.7t'}^{t'} \left[\Delta k_{\mathrm{eq}}(a)\right]^{-m} da\right] \tag{11}$$

where 0, 0.025, 0.05, …, and 0.7, are arbitrarily chosen and represent the values of the normalized kink length *a*/*t*, at which the local stress intensity solutions are available (e.g., by referencing Figs. 8 and 9). The variable $t'$ is the actual crack growth distance ($t' = t/\sin|\alpha|$). In the case of $\alpha = -90°$such as in Fig. 7, $t' = t$.

The material constants, $C = 6.89 \times 10^{-9} \frac{mm/cycle}{(MPa\sqrt{m})^m}$ and $m$ =3, for ferritic-pearlitic steels listed in Dowling (1998) are used to estimate the fatigue lives. The fatigue lives predicted by Eq. (11) with the use of the complete solutions $k_{\mathrm{I}}$ (Fig. 8) and $k_{\mathrm{II}}$ (Fig. 9) are shown in Fig. 10. Note that the global stress intensity factors $K_{\mathrm{I}}$ and $K_{\mathrm{II}}$ are implicit in Figs. 8 and 9 through the normalization factor $(k_{\mathrm{I}})_0$ (Eq. (7)). In addition, the effect of the load ratio ($R$) is ignored when the range of the stress intensity factor ($\Delta k_{\mathrm{eq}}$) is used in Eqs. (9) and (11). The load ratio is actually 0.2 in the fatigue experiments but is not expected to have significant impacts on the fatigue life estimations of these laser welds.

### *4.3 Simplified Fatigue Crack Growth Model*

In a simplified model, the local stress intensity factors $(k_{\mathrm{I}})_0$ and $(k_{\mathrm{II}})_0$ in Eqs. (7) and (8) are used with the Paris law (Eq. 9). Note that the stress intensity factor solutions are valid only as the kink length $a$ approaching to 0. As treated by Newman and Dowling (1998) and Lin et al. (2006), the ranges of the equivalent local stress intensity factors are assumed to be constant for all kink lengths and are assumed to

be equal to those for the kinked cracks with vanishing length ($a \to 0$). For this simplified model, the fatigue life of a laser weld can then be obtained by substituting Eqs. (7) and (8) into Eq. (9). By direct integration,

$$N = \frac{t'}{C\left(\left(\Delta k_{\text{eq}}\right)_0\right)^m} \tag{12}$$

where $\left(\Delta k_{\text{eq}}\right)_0$ is the range of the equivalent stress intensity factors at vanishing kink length. The fatigue life prediction curve (i.e., Eq. (12)) obtained from this simple approach is plotted in Fig. 10. Again, the effects of the load ratio ($R$) are ignored.

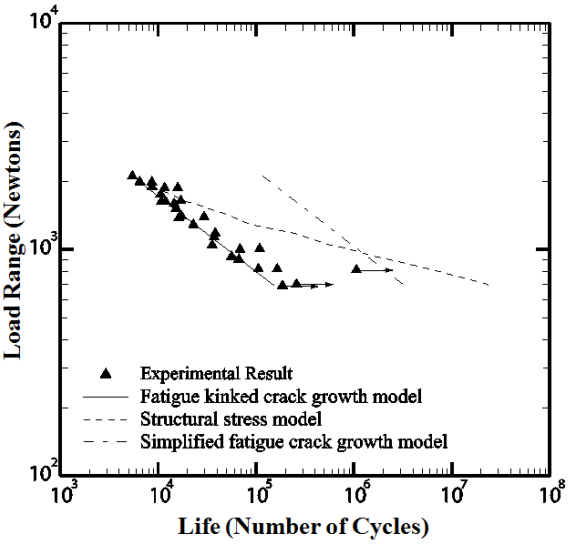


Figure 10: The experimental results and the fatigue life estimations based on the (1) structural stress model, (2) fatigue crack growth model, and (3) simplified fatigue crack growth model.

## 5 Discussions

Figure 10 shows the experimental results of the $CO_2$ laser welded lap-shear specimens made from SAE J2340 300Y HSLA steel. It also includes the fatigue life estimations based on (1) the structural stress (Section 4.1), (2) the fatigue crack growth model (Section 4.2), and (3) the simplified fatigue crack growth model (Section 4.3). It can be seen that the fatigue life estimations based on the fatigue crack

growth model (with the global and the local stress intensity factor solutions for $w/t$= 0.86) are in agreement with the experimental results, while the fatigue lives estimated with the simplified fatigue crack growth model are consistently higher than the experimental data. This is understandable because the value of the equivalent local stress intensity factor increases as the kink length becomes longer, but in the simplified model this quantity is assumed to remain at its initial value evaluated at nearly zero kink length and is lower than the realistic value, which implies a slower crack growth rate and a longer fatigue life.

The solutions of $k_{\mathrm{I}}$ and $k_{\mathrm{II}}$ in Section 3.3.2 for a finite kinked crack can be further improved by considering the actual weld configuration (Fig. 2) to include the weld bead in the finite element model (Fig. 11). As shown in Asim et al. (2014), with the weld bead, the solution for $k_{\mathrm{I}}$ for the right main crack becomes higher than that for the left main crack, but on the other hand, $k_{\mathrm{II}}$ is higher on the left side. Because the absolute value of $k_{\mathrm{II}}$ is only about 10% of $k_{\mathrm{I}}$, the range of the equivalent stress intensity factor $\Delta k_{\mathrm{eq}}$ remains higher at the right kinked crack. This suggests that the right kinked crack should grow faster and the failure would occur first in the right side of the lap-shear specimen. Indeed this is consistent with the experimental observation for high cycle fatigue testing [Asim et al. (2014)] and is shown in Fig. 3.

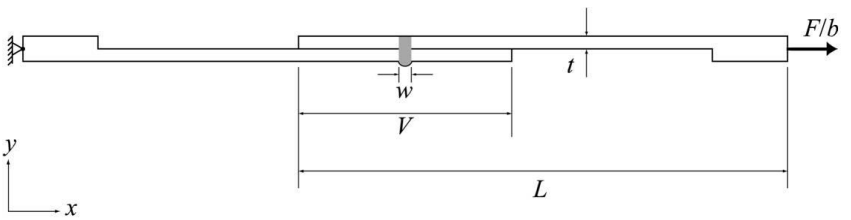


Figure 11: A schematic of a two-dimensional finite element model of a lap-shear specimen with a weld bead.

It is well known that the Paris Law typically well represents the fatigue crack growth behavior in most of the stress intensity factor ($\Delta K$) range, however, it would overestimate *da/dN* at the initial or threshold $\Delta K$ and underestimate it at large $\Delta K$. An alternative formulation based on the method of Moving Least Squares, or MLS, [e.g., see Atluri and Zhu (1998); Kim and Atluri (2000)] to model fatigue behavior in terms of $\Delta K$ was proposed by Dong et al. (2015). These researchers demonstrated that only very few MLS nodes were needed to predict the *a vs. N* or the *da/dN vs.* $\Delta K$ curves very accurately for 7075-T6 aluminum alloy, where $\Delta K$ was obtained by the Finite Element Alternating Method (FEAM) as was shown by Nish-

ioka and Atluri (1983) and Dong and Atluri (2013a; 2013b). In a more recent work by Wang et al. (2015), they introduced probabilistic frame work with Kalman and particle filters to remove the errors caused by experimental noises, for example, from the experimental *a vs. N* data set. Such treatment allows the mean value and probabilistic distribution of the remaining useful life be calculated. It would be interesting to implement MLS in the study of the kinked fatigue crack growth such as the present work in the case of a lap-shear joint.

## 6 Conclusions

This paper summarizes part of the research at the University of Michigan on predicting the fatigue lives of lap-shear specimens based on fracture mechanics. A full range of approximate closed-form solutions for global stress intensity factors are first developed for the main crack based on the results of (1) finite element analyses in conjunction with (2) analytical solutions with beam bending theory and (3) Westergaard stress function solutions for two semi-infinite solids which share a common boundary with a length equal to the size of the weld. It is followed by a series of finite element analysis to calculate the local stress intensity factors at the tip of the kinked crack emanating from the main crack tips. The computational results indicate that the kinked cracks are under dominant Mode I loading ($k_{\mathrm{I}} >> k_{\mathrm{II}}$). Combining the calculated local stress intensity factors with the global stress intensity factors ($K_{\mathrm{I}}$ and $K_{\mathrm{II}}$), the fatigue life of laser welded lap-shear specimen can be estimated. In addition, a standard engineering practice of using the structural stress and the $S-N$ curve to predict the fatigue lives is also presented. Comparing with the fatigue test data of the lap-shear specimens, it can be concluded that the fatigue lives estimated with the kinked fatigue crack growth model agree well with the experimental results, whereas the estimations based on the structural stress agree only at higher fatigue loads.

## References

**Asim, K.; Sripichai, K.; Pan, J.** (2014): Fatigue behavior of laser welds in lap-shear specimens of high strength low alloy steel sheets. *Int. J. Fatigue*, vol. 61, pp. 283–296.

**Atluri, S. N.; Zhu, T.** (1998): A New Meshless Local Petrov-Galerkin (MLPG) Approach to Nonlinear Problems in Computer. *Modeling & Simulation, Computer Modeling & Simulation in Engg.,* vol. 3, pp. 187-196.

**Bilby, B. A.; Cardew, G. E.; Horward, I. C.** (1978): Stress intensity factors at the tip of kinked and forked cracks. *The fourth international conference on fracture*, University of Waterloo, Ontario, June 19-24, 1977; Pergamon Press, New York,

3A, pp. 197-200.

**Cotterell, B.; Rice, J. R.** (1980): Slightly curved or kinked cracks. *Int J Fract*, vol. 16, pp. 155-169.

**Dong, L.; Atluri, S.N.** (2013a): Fracture & Fatigue Analyses: SGBEM-FEM or XFEM? Part 1: 2D Structures. *CMES: Computer Modeling in Engineering & Sciences,* vol. 90, pp. 91-146.

**Dong, L.; Atluri, S.N.** (2013b): Fracture & Fatigue Analyses: SGBEM-FEM or XFEM? Part 2: 3D Solids. *CMES: Computer Modeling in Engineering & Sciences,* vol. 90, pp. 379-413.

**Dong, L.; Haynes, R.; Atluri, S. N.** (2015): On Improving the Celebrated Paris' Power Law for Fatigue, by Using Moving Least Squares. *CMC: Computers Materials and Continua,* vol. 45, pp. 1-15.

**Dowling, N. E.**, (1998): *Mechanical Behavior of Materials, Second Edition*, Prentice Hall, New Jersey.

**Kim H. G., Atluri, S. N.** (2000): Arbitrary placement of secondary nodes, and error control, in the meshless local Petrov-Galerkin (MLPG) method. *CMES-Computer Modeling in Engineering & Sciences,* vol. 1, pp. 11-32.

**Lin, P. C.; Pan, J.** (2008): Closed-form structural stress and stress intensity factor solutions for spot welds in commonly used specimens. *Eng Fract Mech*, vol. 75, pp. 5187-5206.

**Lin, S. H.; Pan, J.; Wung, P.; Chiang, J. A.** (2006): A fatigue crack growth model for spot welds under cyclic loading conditions. *Int J Fatigue*, vol. 28, pp. 792-803.

**Lin, P. C.; Wang, D. A.; Pan, J.** (2007): Mode I stress intensity factor solutions for spot welds in lap-shear specimens. *Int J Solids Struct*, vol. 44, pp. 1013-1037.

**Nishioka, T.; Atluri, S. N.** (1983): An Alternating Method for Analysis of Surface flawed Aircraft Structural Components. *AIAA Journal,* vol. 21, pp. 749-757.

**Newman, J. A.; Dowling, N. E.** (1998): A crack growth approach to life prediction of spot-welded lap joints. *Fatigue Fract Engrg Mater Struct*, vol. 21, pp. 1123-1132.

**Radaj, D.** (1989): Stress singularity, notch stress and structural stress at spot – welded joints. *Eng Fract Mech*, vol. 34, pp. 495-506.

**Radaj, D.; Zhang, S.** (1991a): Stress intensity factors for spot welds between plates of unequal thickness. *Eng Fract Mech*, vol. 39, pp. 391-413.

**Radaj, D.; Zhang, S.** (1991b): Simplified formulae for stress intensity factors of spot welds. *Eng Fract Mech*, vol. 40, pp. 233-236.

**Radaj, D.; Zhang, S.** (1992): Stress intensity factors for spot welds between plates

of dissimilar materials. *Eng Fract Mech*, vol. 42, pp. 233-236.

**Sripichai, K.; Asim, K.; Pan, J.** (2011): Stress intensity factor solutions for estimation of fatigue lives of laser welds in lap-shear specimens. *Eng Fract Mech*, vol. 78, pp. 1424-40.

**Tada, H.; Paris, P. C.; Irwin, G. R.** (2000): Infinite planes with two semi-infinite cracks (page 4-11) in *The stress analysis of cracks handbook. 3rd Edition,* New York, ASME Press.

**Wang, H.; Haynes, R.; Huang, H.; Dong, L.; Atluri, S. N.** (2015): The Use of High-Performance Fatigue Mechanics and the Extended Kalman / Particle Filters, for Diagnostics and Prognostics of Aircraft Structures. *CMES: Computer Modeling in Engineering & Sciences,* vol. 105, pp.1-24.